efficiently all the way to the outer surface. Note the relatively large errors on measurements as the films are quite rough and their thickness difficult to determine with high precision.

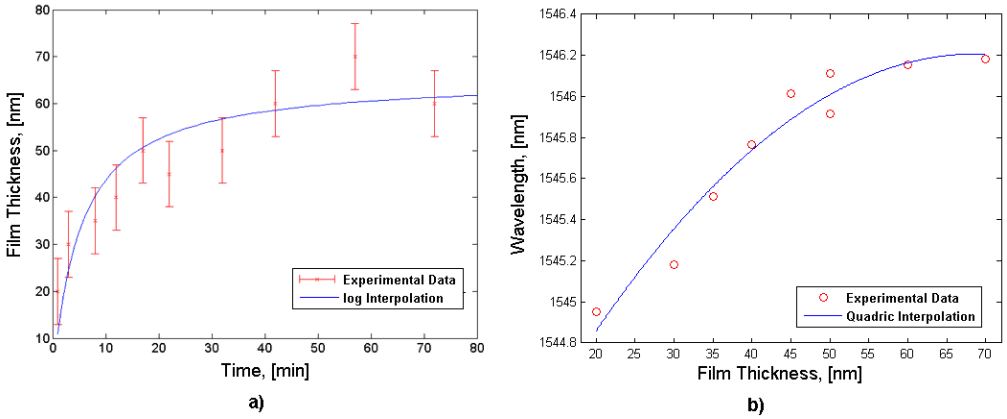

Fig. 6. (a) Time evolution of the average gold film thickness extracted from AFM measurements on individual samples. (b) Correlation between the film thickness and the optical response of the sensor acquired at the P_y polarization state at 1545 nm wavelength.

Before moving on to the thickness optimization results, the film morphology was studied with scanning electron microscopy (Fig. 7).

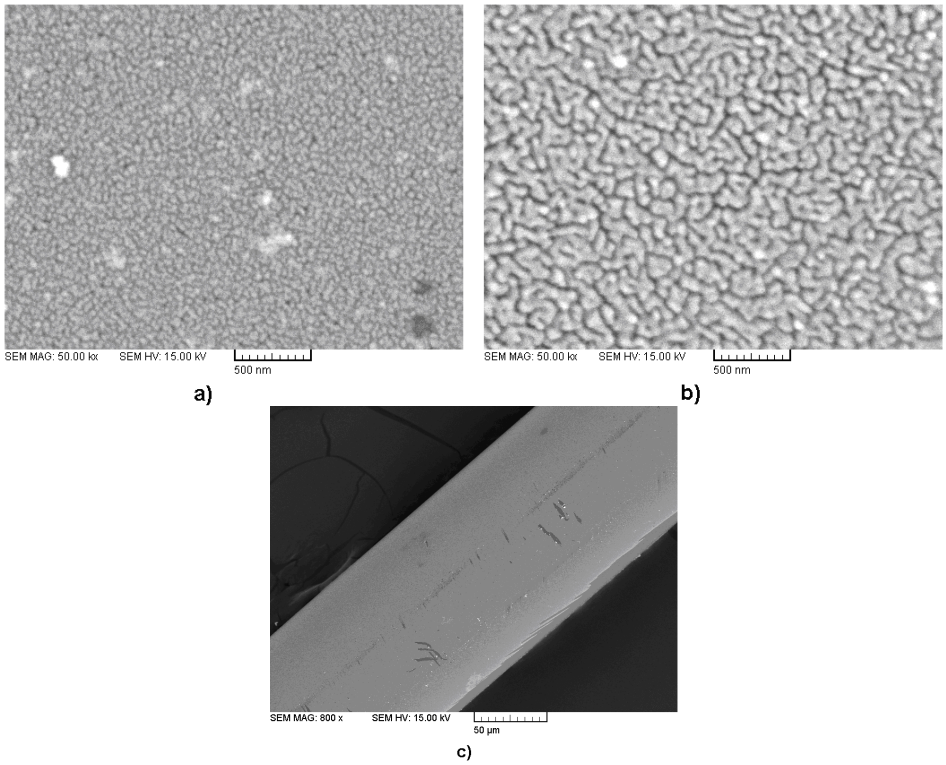

Fig. 7. SEM images of electroless gold plating of the fiber's surface. (1) after 1 min of deposition (2) after 45 min of deposition, (c) image of the fiber's circumference after 40 min of deposition.

The shape of the initial gold particles is spheroid but during electroless plating the metal coating assumes a complex structure with an agglomeration of randomly interconnected plates

#151467 - $15.00 USD Received 20 Jul 2011; revised 27 Aug 2011; accepted 27 Aug 2011; published 12 Sep 2011

that have relatively large (100s of nm) lateral dimensions relative to the overall film thickness (about 40 nm for Fig. 7(b)). The RMS surface roughness of the final films is 5.17 nm

In spite of this small scale granularity (and some physical scratches that were made after deposition on this sample) a larger scale image (Fig. 7(c)) shows that the deposited film coats the fiber surface uniformly. The question now arises whether these films can support surface plasmons that have sufficient quality to be used in sensing applications.

3.2 Thickness optimization

Although the techniques presented above can be calibrated to monitor the film growth, it is quite obvious that they are not precise enough to obtain the optimal film thickness for SPR excitation. To overcome this problem a second technique based on a different analysis of the full TFBG spectrum envelope has been developed.

As shown in an earlier publication [21], the information from the two orthogonal polarizations P_x and P_y can be combined in a single spectrum by introducing the Polarization Dependent Loss (PDL) parameter defined as:

$$PDL(\lambda) = \left| 10Log_{10}\left(\frac{T_x(\lambda)}{T_y(\lambda)}\right)\right| \quad (1)$$

where T_x, and T_y are the transmission spectra for the P_x and P_y polarization states. It was demonstrated that when the metal coating has a thickness for which a plasmon wave can be excited by cladding modes, the PDL spectrum acquires a deep "notch" that reveals the SPR location, and that can be monitored in sensing applications. We now use this characteristic feature of the PDL spectrum to identify the precise moment of the plating process at which the SPR signature is optimized. When the spectral notch is maximized, the thickness is optimal for SPR operation.

This is best observed in the density plot of Fig. 8, where the envelopes of the PDL spectra are represented as a colour scale in the horizontal direction and different plating times (vertical direction). These spectra were obtained in a different experiment from the one reported in the preceding section (although the results of that section could have been processed in the same manner). The chemical concentrations used as well as the size of the plating bath were somewhat larger in the second experiment, resulting in faster plating rates. Indeed, it can be clearly seen that after only approximately 7 min of gold film deposition a deep notch in the PDL envelope occurs (darkest blue colour in Fig. 8(a)). The individual PDL spectrum corresponding to this plating time is shown as Fig. 8(b), while Fig. 8(c) extracts the time evolution of the PDL value at the wavelength where the SPR is observed. The optimum point is clearly seen in the latter figure and provides a tool to interrupt the plating process as soon as a local PDL envelope minimum is reached, regardless of the plating rate. A movie showing the time evolution of the actual PDL spectra is also provided to illustrate more clearly how strongly and suddenly the SPR signature appears during the plating. Figure 8(c) further shows that the PDL envelope evolution slows down gradually for longer plating times (similar to the behavior of the individual loss resonances observed in the first experiment). These effects are due to both the self-termination of the plating process and to the fact that as the metal layer becomes thicker it eventually shields the light from the cladding modes from the outside medium so that further thickness growth is not detected.

#151467 - $15.00 USD Received 20 Jul 2011; revised 27 Aug 2011; accepted 27 Aug 2011; published 12 Sep 2011

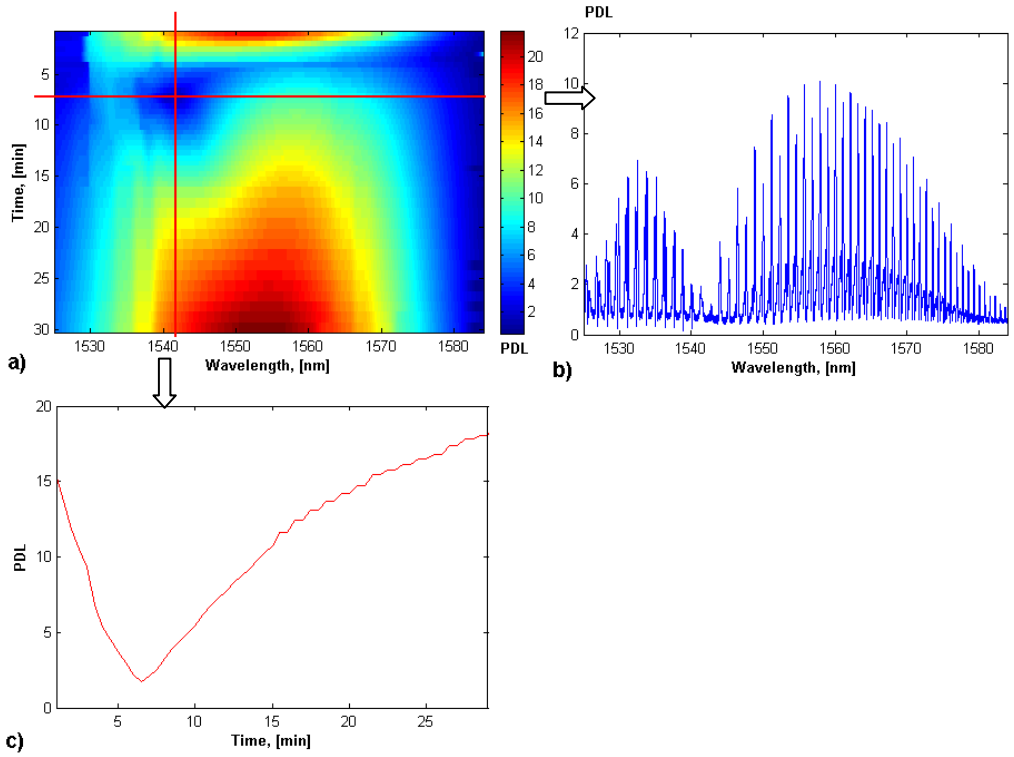

Fig. 8. (a) The envelope of PDL spectra, taken continuously along the course of gold film deposition, and cross sections centered at the point of the deepest notch: wavelength = 1542 nm (b) and time = 7 min (c). (Media 1) The time-lapse evolution of Fig. 8(b) during plating.

4. Conclusion

Electroless plating of gold on optical fibers using nanoparticle seeds attached to the fiber followed by reduction of gold from chloroauric acid in solution has been demonstrated. Plating is a batch process in which large numbers of devices can be coated simultaneously. Plating is also a conformal process, whereas all exposed surfaces of the same material in the plating bath are coated simultaneously and uniformly. Therefore, plating is an ideal method to coat optical fibers with nanoscale layers of metals. Here, gold films with sufficient thicknesses (40 to 60 nm) and uniformity for the realization of fiber SPR sensors have been obtained. Using Tilted Fiber Bragg gratings, we have presented two methods to monitor the growth of the plated film in situ and in real time. The time evolution of the resonance wavelengths of certain cladding modes has been shown to follow the growth of the film thickness. Most importantly however, we showed that by monitoring a simple parameter in the Polarization Dependent Loss of the TFBG during plating, the optimum film thickness for SPR operation can be found with great accuracy, regardless of the plating rate. Obviously this method only applies to the optimum conditions for SPR in water solutions (i.e. similar to the plating bath), and at the wavelengths where the interrogation is carried out. However these conditions are fairly typical for fiber SPR sensor applications in general. It must be pointed out that although we used the TFBG-SPR platform [21] to perform these experiments the monitoring and optimization process can be applied to other types of fiber SPR devices (such as those in [11]) since plating is a batch process in which the TFBG could be inserted amongst other kinds of sensors being plated simultaneously. It is also likely that other metals could be plated and monitored in similar fashion. The method is inherently limited in thickness since the evanescent field of the cladding modes must tunnel across to the outer surface of the metal

#151467 - $15.00 USD Received 20 Jul 2011; revised 27 Aug 2011; accepted 27 Aug 2011; published 12 Sep 2011

film in order to detect changes in thickness. When the thickness exceeds the penetration depth of the light, the thickness growth appears to saturate. Obviously for the application of fiber SPR, the thickness needed must be smaller than the penetration depth, so this does not present an actual limitation in this case. For each type of metal coating, it is possible to predict the optimum SPR thickness and the resulting SPR wavelength with very good accuracy by using planar models (such as the one described in [30]) because the outside surface of the fiber has a radius of curvature that is large relative to the wavelength.

One last observation is that the plated films are relatively rough on the scale of their thickness (RMS roughness close to 10% of the thickness), but that a high quality SPR signature was obtained nevertheless.

Acknowledgments

Financial support from NSERC, the Canada Research Chairs program, and the Institut National d'Optique (Québec) is gratefully acknowledged. C. Caucheteur is supported by the Belgian F.R.S.-FNRS.

#151467 - $15.00 USD Received 20 Jul 2011; revised 27 Aug 2011; accepted 27 Aug 2011; published 12 Sep 2011